Univerzita Karlova v Praze
Matematicko-fyzikální fakulta

BAKALÁŘSKÁ PRÁCE

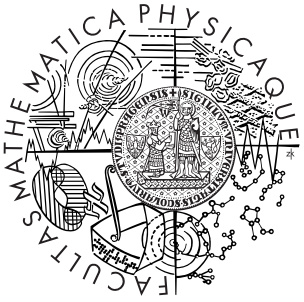

Peter Petrík

Návrh optimální numerické metody pro řešení Rayleigh-Plessetovy rovnice s prudkými kavitačními kolapsy

Matematický ústav UK

Vedoucí bakalářské práce: Prof. Ing. Maršík František, DrSc.
Studijní program: Obecná fyzika

2008

Chtěl bych poděkovat Prof. Ing. Františekovi Maršíkovi, DrSc., že mi umožnil psaní této práce v zahraničí.

Prohlašuji, že jsem svou bakalářskou práci napsal samostatně a výhradně s použitím citovaných pramenů. Souhlasím se zapůjčováním práce a jejím zveřejňováním.

V Praze dne 11.5.2008 Peter Petrík

Contents

Název práce: Návrh optimální numerické metody pro řešení Rayleigh-Plessetovy rovnice s prudkými kavitačními kolapsy
Autor: Peter Petrík
Katedra (ústav): Matematický ústav UK
Vedoucí bakalářské práce: Prof. Ing. Maršík František, DrSc.
e-mail vedoucího: marsik@it.cas.cz

Abstrakt: V práci studujeme přesnost a časovou náročnost jednokrokových explicitních metod (Runge-Kutta, Bulirsch-Stoer) s adaptabilním krokem v Rayleigh-Plessetově rovnici, která popisuje vývoj poloměru plynné bubliny v kapalině se změnami tlaku. Metody podceňují lokální chybu v místech kolapsů bublin, avšak globální chyba zůstáva v řádu použité tolerance. Bulirsch-Stoer metoda vykázala nejmenší časovou náročnost. V případě Runge-Kutta metod závisí výběr optimální metody na použité toleranci. Při středních tolerancích urychluje výpočet i použití regularizace, tj. zavedeni nové nezávislé proměnné místo času. Časová náročnost použité metody se mění s různými použitými variantami rovnice (izotermická aproximace/adiabatická aproximace plynné složky obsahu bubliny, stlačitelná/nestačitelná kapalina). Pri některých nastaveních vstupních parametrů v izotermické variantě rovnice dochází k pádu výpočtu (poloměr bubliny je nereálně malý). Tento pád sa nedá odstranit použitím odlišného kritéria na toleranci numerické metody. Při potřebě velkého množství výpočtů Rayleigh-Plessetovy rovnice navrhujeme proto používat regularizovaný tvar a Bulirsch-Stoerovu metodu.
Klíčová slova: Rayliegh–Plesset;Runge-Kutta ; numerické metody; bublina

Title: Suggestion of an optimal numerical method for solution of the Rayleigh-Plesset equation with rebounding
Author: Peter Petrík
Department: Mathematical Institute of Charles University
Supervisor: Prof. Ing. Maršík František, DrSc.
Supervisor's e-mail address: marsik@it.cas.cz

Abstract: In the work we study stability and time effectivity of explicit one-step methods (Runge-Kutta, Bulirsch-Stoer) with adaptible step size for Rayleigh-Plesset equation, which describes the evolution of radius of bubble in the liquid with changing pressure. Methods underestimate local error in places of collapses of bubble, but global error stays in order of used tolerance. The Bulirsch-Stoer method has the lowest time demands. In case of the the Runge-Kutta Methods selection of optimal method depends on used tolerance. In case of middle tolerance level one can accelerate computation by use of regularization (proposing new independent variable instead of time). The efficiency of each numerical method depends on the variant of the equation (adiabatic/isothermal approximation of the gas, the liquid compressibility). In some settings of initial parameters of the equation computation even falls (unreasonably small radius). In case of large amount of computation of the Rayleigh-Plesset equation we suggest to use the regularized form with Bulirsch-Stoer Method.
Keywords: Rayliegh–Plesset; Runge-Kutta ; numerical methods; bubble

1 Introduction

In this paper, we use numerical methods (the explicit Runge-Kutta and the Bulirsch-Stoer method) to solve the highly non-linear, ordinary differential the Rayleigh-Plesset equation. Virtually all of the *spherical bubble* models are based on some version of the Rayleigh-Plesset equation that defines the relation between the radius of a spherical bubble, and the pressure in the the liquid far from the bubble.

Consider the following situation. A gas bubble is traveling with a the liquid in a pump. When the bubble comes near the blade of the pump, the pressure in the the liquid changes quickly, which causes the bubble to expand and then contract violently, overshooting its equilibrium size. With the lowering of the radius in the bubble, the pressure (and the temperature) inside increases, which causes *collapse* or *rebound* of the bubble. This phenomenon is closely related to the problems of *cavitation*, which can be defined as a "breakdown [1] of a the liquid medium under very low pressures[2]"[2, p.1].

Bubble collapses are frequently found in practice. Cavitation damage, cavitation noise, sonochemistry, shock wave lithotripsy, ultrasonic imaging and sonoluminescence are examples of technological and scientific applications, in which bubble collapses play a central role.

Perhaps the most common engineering problem caused by cavitation is the material damage. *Cavitation damage* refers to the phenomenon that can be described as follows: "Strong pressure variations in the the liquid are produced by the jet and the shock emitted after the bubble collapses. The combined effect of several bubbles undergoing this process is believed to cause erosion in nearby solids."[7].

Figure 1.1: Photograph of pump damage caused by cavitation erosion[4]. Courtesy of Sigma Lutín

[1] Creation of vapor cavities
[2] Below vapor pressure

Large amount of computation of the Rayleigh-Plesset equation for various initial conditions is needed inside the numerical solver of 3-D Navier-Stokes equations with turbulence for pump, which performance is simulated in SIGMA Research & Development Institute, Ltd. The aim of the simulation is to predict the position and extent of the material damage at blades. The damage is calculated from the change of radius and pressure in the bubble during the first few collapses.

Thus it is necessary to find a *stable* and *effective* numerical method for computation of the Rayleigh-Plesset equation and a suitable physical model (consistent with the experimental data gained from the tested pump (Fig. 1.1). A very fast bubble collapse often causes failure of the computation for the non-compressible isothermal model and the Runge-Kutta-Fehlberg-45 method (RKF45[3]). Details of computation of damage and simulation can be found in [4]. This work on finding the optimal numerical method (in the sense of stability and speed) was motivated by the grant number 101/07/1612 of the Czech Science Foundation entitled "Influence of physical properties of water to nucleation of bubbles and cavitation damage in pumps.".

In this paper, we focused on the *Runge-Kutta* family of methods and the *Bulirsch-Stoer method*, and tested them in terms of speed and stability. According to [9, p.709]:

> "The relatively simple Runge-Kutta and Bulirsch-Stoer routines we give are adequate for most problems. Runge-Kutta succeeds virtually always; but it is not usually fastest, except when evaluating right side is cheap and moderate accuracy ($< 10^{-5}$) is required. However, predictor-corrector methods are for many smooth problems computationally more efficient than Runge-Kutta, but in recent years Bulirsch-Stoer has been replacing predictor-corrector in many applications."

The best method can be applied in the numerical solver used in Sigma to increase the efficiency and speed of the computation.

There is a large number of different mathematical models that describe the dynamics of a single spherical bubble. From the simple ODEs (the Rayleigh-Plesset equation) to the complex system of PDEs (the Navier-Stokes equations). There are compared in various works, e.g. [7] or [1] , [2] , [3]. In chapter "Remarks on Different Models" we discuss the stability of the numerical methods with respect to different variations of the Rayleigh-Plesset equation (isothermal (gas)-non compressible (the liquid) model, isothermal-compressible model and adiabatic-non-compressible model). It is not the goal of this paper to discuss the physical differences between those models, or to choose the best model for the 3-D numerical solver of pump used by SIGMA institute. In contrast, our objective is to find the optimal numerical method for solving these models. The selection of the best suitable model must be made with respect to the experimental data. As shows the work of Goldsztein [7], the models with exchange of heat energy (radiation, convection, ...) are better than simple adiabatic/isothermal models.

[3]For use of abbreviations see B.1

2 Tested Model

2.1 The Rayleigh-Plesset Equation

Used Rayleigh-Plesset equationdescribes spherical bubble from *ideal* the gas inside *incompressible* viscous still the liquid (for the derivation see Appendix A), which undergoes pressure changes in the infinity.

$$\frac{d^2R}{dt^2} = -\frac{1}{R}\left(\frac{3}{2}\left(\frac{dR}{dt}\right)^2 + \frac{4\mu}{R}\frac{dR}{dt} + \frac{2\sigma}{\rho R} - \frac{p_v + p_g - p_\infty}{\rho}\right) \tag{2.1}$$

where $p_v = 2339Pa$ is the equilibrium pressure inside the bubble, p_g is pressure of the gas in the bubble, $c = 1550ms^{-1}$ is the initial speed of light in the liquid,κ is the polytropic coefficient, $\sigma = 0,0727Nm^{-1}$ is the surface tension, $\mu = 0,001Pa \cdot s$ is the dynamic viscosity, $\rho = 1000kg \cdot m^3$ is the initial density of the liquid

Total pressure in the bubble p_B is thus given by:

$$p_B = p_v + p_g \tag{2.2}$$

We assume that the gas inside the bubble is ideal:

$$p_g = p_{g0}\left(\frac{R_0}{R}\right)^{3\kappa} \tag{2.3}$$

where R_0 is the starting radius of the bubble and $\kappa = 1$ (*isothermal* approximation) is the polytropic coefficient .

Further:

$$p_{g0} = p_{atm} + \frac{2\sigma}{R_0} - p_v \tag{2.4}$$

where $p_{atm} = 101300Pa$ is the atmospheric pressure.

We used the initial radius $R_0 = 4 \cdot 10^{-3}$ and initial change of the radius $\frac{dR}{dt} = 0$ if not said elsewere. Bubble radius R was calculated to time $tmax = 2,7 \cdot 10^{-2}$ (for characteristic shape of solution see (Fig. 3.2))

2.2 Typical Pressure in the Infinity

The pressure in infinity is given by approximation of the typical pressure in the pump from 3D numerical solver (comparison at (Fig. 2.1)) by the analytical function:

$$p_\infty = \frac{-54\arctan\left(5000(t-0,0120)\right)\arctan(1000(t-0,0125))}{(t-0,0125)} + 58000; \tag{2.5}$$

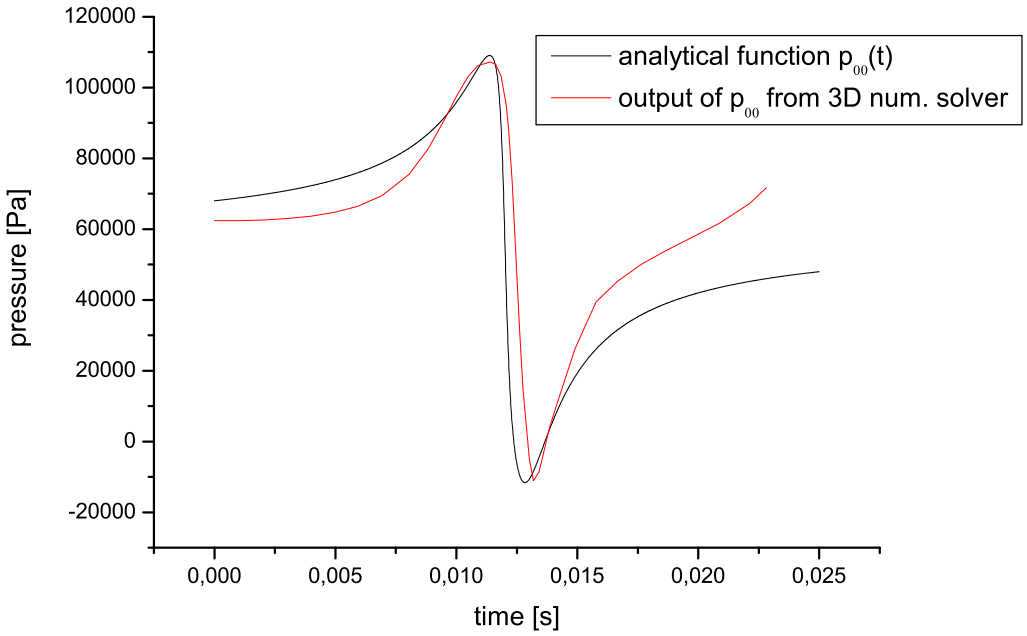

Figure 2.1: Pressure in infinity

3 Evaluation

3.1 Reduction, Scaling, Regularization

The Rayleigh-Plesset equation is initial value problem; conditions of the equation are specified at the start. In this paper we use only methods, which are explicit and one-step.

According to work of Lastman and col. [8]: "The eigenvalues of Jacobian matrix of the right side Rayleigh-Plesset equation (2.1) are complex, with real and imaginary parts approximately $\pm 10^{13}$, and hence system is *not stiff*. However, near collapse points small integration steps are required to maintain integration accuracy."

The generic problem of ODEs can always be reduced to system of first-order differential equations. We use these reductions:

1. With (2.1) we use "*normal*" reduction

$$\frac{dR}{dt} = B \tag{3.1}$$

2. We tried also *non-dimensional* form of the Rayleigh-Plesset equation from [2, p.48], with same reduction (3.1), but with proposing new variables:

$$\overline{R} = \frac{R}{R_0}$$

$$\overline{t} = \frac{t}{\tau}$$

$$\overline{p} = \frac{\overline{P_0}}{P}$$

with characteristic time scale $\tau = a \cdot \sqrt{\frac{\rho}{P}}$ and characteristic pressure difference $P = 2 \cdot p_{atm}$ The equation (2.1) then takes form:

$$\frac{\overline{dB}}{dt} = -\frac{1}{\overline{R}}\left(\frac{3}{2}\left(\overline{B}\right)^2 + \frac{We}{\overline{R}} + \frac{\overline{B}}{\overline{R} \cdot Re} - Th\frac{p_v - p_\infty}{P} - \frac{\overline{P_0}}{\overline{R}^{3\kappa}}\right) \tag{3.2}$$

where $Re = \frac{R_0^2 \rho}{4\mu\tau}$ is Reynolds number, $We = \frac{2\sigma\tau^2}{\rho R_0^3}$ is Weber number and $Th = \frac{P\tau^2}{\rho R_0^2}$ and $\overline{P_0} = \frac{p_{g0}\overline{R_0}^{3\kappa}\tau^2}{\rho R_0^2}$ are pressure numbers

3. Motivated by work [8], we tried also *regularization*:

$$\frac{dt}{ds} = \frac{R^2}{R_0^2} \tag{3.3}$$

$$\frac{dR}{dt} = \frac{BR^2}{R_0^2} \tag{3.4}$$

$$\frac{dB}{dt} = \frac{R}{R_0^2}\left(-\frac{3}{2}(B)^2 + \frac{p_v + p_g - p_\infty}{\rho}\right) - \frac{1}{R_0^2\rho}(4\mu B + 2\sigma) \tag{3.5}$$

The results can be seen in Appendix C (Tab. C.4). Non-dimensional form (3.2) produced negligible increase of number of evaluation of right side (nE) of Rayleigh-Plesset equation (0,08%) and also negligible difference in global error. On the other hand **regularization increased speed of the calculation** (by 48%) with medium tolerance level ($\epsilon = 10^{-4}$), but with higher tolerance ($\epsilon \sim 10^{-8}$ and more), the difference between these 3 methods is minimal. In the work of Lastman, Wentzell and Hindmarsch [8], they investigated the impact of different regulariations and integrators with respect to the number of nE (medium tolerance $\epsilon = 10^{-4}$) .The fastest regularization solved Rayleigh-Plesset equation with $nE = 870$, fastest integrator EPISODE (based on the variable- step multistep formulas) of non-regularized equation with $nE = 1768$ steps.

3.2 Used Tolerance Criterium

We use this general criterium for accepting next step:

$$\epsilon > max\left(\frac{ErrR}{R}, \frac{ErrB}{B}\right) \tag{3.6}$$

or in case of the embedded methods (and the euler's method):

$$\epsilon > \left(\frac{ErrR}{R}\right) \tag{3.7}$$

where $ErrR$ and $ErrB$ are estimated errors of R and B respectively.

We investigated difference between use of (3.6) and (3.7). The result is that (after successful computation) the difference is time and accuracy is minimal (negligible). The reason is that $\frac{ErrR}{R} >> \frac{ErrB}{B}$ is the most cases (because $R \to 0$ in case of collapse). The opposite situation occurs only when $B \doteq 0$, but that means that R is not changing and hence it does not have impact on accuracy. However, use of

criterium (3.6) causes failure of the Euler's methods and in some cases also others methods, because the condition $\epsilon > \frac{ErrB}{B}$ cannot be fulfilled. In general case, there is possibility that change of B is very radical in some part of the computation (e.g. radical change of the pressure in the infinity - see (Fig. 2.1) at point $t = 0,120s$) and then use of (3.7) can lead to wrong solutions. Hence it is suitable to use (3.6, and after failure of the computation try (3.7) with increased attention. Other possibility is to use different criterium for accepting current step (see [9, p. 881]), e.g. based on current step size h (however in the point of collapse in our settings, $h \sim 10^{-14}$ and $R \sim 10^{-7}$, hence criterium (3.6) is better). There is also the possibility proposed by Schampine [11] to use criterium with relative to largest value of R during computation, but we need to use method for bubbles with different initial radiuses and hence with different largest values (range depends on pressure in the infinity and used range of the bubbles), so it should be necessary set a rather stringent tolerance to avoid non-physical solutions (e.g. $R < 0$). With our settings (3.6) and $\epsilon \geq 10^{-4}$, the situation $R < 0$ never occurred, but integration is successful only with small range of initial radius of the bubble (see chapter "Different models"). When the failure of computation with (3.7) occurred (e.g. $R_0 = 10^{-4}$), we tried to put some criterium with absolute value *abs*:

$$\epsilon > max\left(\frac{ErrR}{R}, \frac{ErrB}{B}, abs\right) \tag{3.8}$$

but the failure of the computation also occurred with error message :"$R < 0$" or "step lowered below 10^-30" (not reliable in double precision), depended on value of *abs*

3.3 Global Error and Local Error

Because the Rayleigh-Plesset equation has no analytical solution, we cannot compare calculated estimated local error (and global error) of used methods directly.

In the work of Alehossein and Qin [5], they compared error estimate and speed of the Euler, central, modified Euler and the RKF method to *simple singular differential equation* with solution $y = \tan(x)$. The Euler method produces the largest error and the RKF45 method produces the smallest error. They also showed, that **constant step methods are not suitable** for this problem. In simple run of the RKF45 , the change of step is in order of 10^{10}!

We used different approach to determine the real error of methods. Imagine that we accepted step R (criterium (3.6) was fulfilled) with size h. For estimating *real local error* we take 50 steps of rkv8 with step $\frac{h}{50}$ (from exactly same local starting point as method used) and thus get approximate solution R_{50} in same time as R. Then we approximate local real tolerance by

$$\epsilon_{loc} = \left(\frac{abs(R_{50} - R)}{R}\right) \tag{3.9}$$

then we can look on ration $\theta = \frac{\epsilon_{loc}}{\epsilon}$. More the ratio is close to 1, the better estimation of local error method has. We calculated max of this ratio during whole calculation θ_{max} and mean (with weight h) $\overline{\theta}$. Further, we use variable real tolerance $\epsilon_{real} = \overline{\theta} \cdot \epsilon$, because different methods use parameter ϵ in different ways (e.g. safety factors, ...).

Results show that **real tolerance ϵ_{real} varies during the integration** (see (Fig. 3.1)). There are 4 places, when the tolerance is above desired level. First is

when the pressure is changing rapidly (see (2.5)), others 3 are places of the bubble collapses. However, Rayleigh-Plesset equation is not stiff and these local peaks above tolerance level do not devalue global solution. Actual height and location of peaks varies greatly with starting values of the integration and method used. Hence we use in next consideration only mean value of these local errors ϵ_{loc}.

Figure 3.1: Comparison of ϵ_{loc} of various methods ($\epsilon_{real} \sim 10^{-6}$)

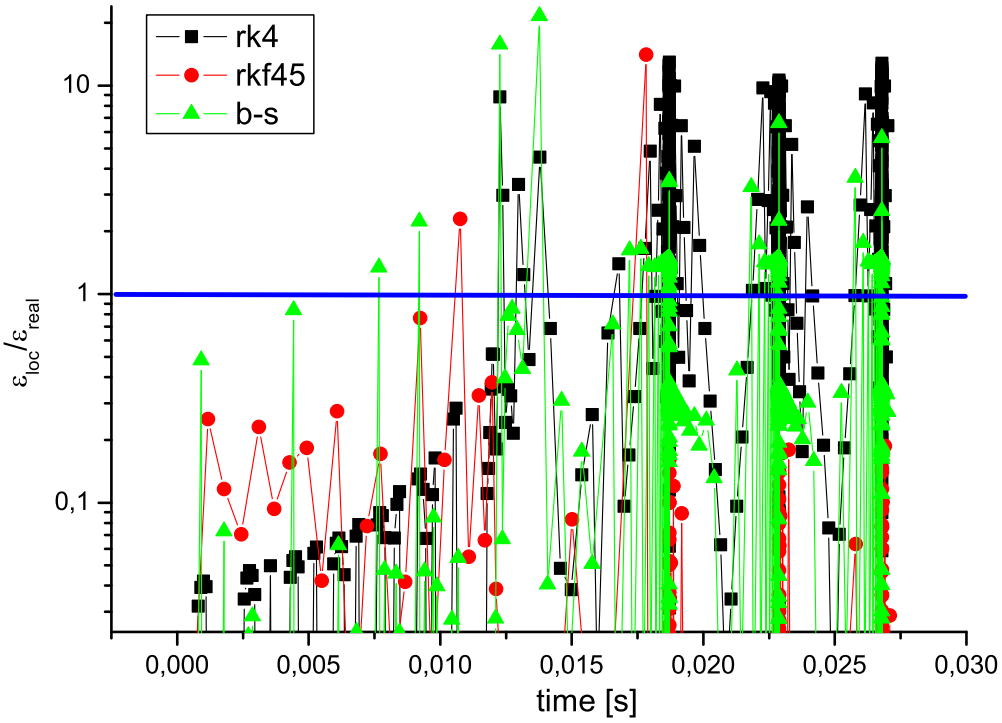

For estimating global error we calculated solution with rkv8, with $\epsilon = 10^{-15}$ and minimum step $h_{min} = 10^{-7}$ (see (Fig. 3.2)). We determined the time position $t_{3ex} = 0,026776868134125772$ of third collapse of bubble and then we compared this number with position t_3 of same collapse calculated by other used methods. The difference $\lambda = abs(t_{3ex} - t_3)$ we took as indicator of global error.

The **ratio of global error and real tolerance** $\omega = \frac{p_\lambda}{p_{\epsilon_{real}}}$ and/or the ratio $\varpi = \frac{\lambda}{\epsilon_{real}}$ **behave as constant**, independently on used method and tolerance (see appendix C, (Tab. C.1)-(Tab. C.3))). Mean values of these variables are: $\overline{\omega} = 1,10 \pm 0,02$ and $\overline{\varpi} = 0,9 \pm 0,2$. This can be caused by non-stiffness of Rayleigh-Plesset equation , and it can be useful in the predictions of the global error in the applications.

3.4 Speed

We used variable nE,number of evaluations of right side of the Rayleigh-Plesset equation , as indicator of speed of the given numerical method. As the global error has same magnitude as the real tolerance, the good indicator of effective method is the graph of nE on dependence of order of used real tolerance (or global error).

We will refer to this comparison as effectiveness of the method. The results can be found in appendix C, and are plotted on (Fig. 3.3) and (Fig. 3.4). There are two conclusions that arose:

1. **Effectiveness** of the classical methods and the embedded methods (see appendix B) **is dependent on used tolerance**. As it can be seen on (Fig. 3.4), RK4 is the most effective method from the classical methods (RK4, RKB6, RKV8) to the order $\lambda \sim 10^{-4}$, but it is the least effective from the order $\lambda \leq 10^{-6}$. Same behavior shows also the embedded methods (RKF45 and RKF78) on (Fig. 3.3), but the breaking point is at $\lambda \sim 10^{-8}$. To sum it up, the optimal method must be chosen with the respect of the used tolerance. A high order method for a high tolerance and a low order method for a lower tolerances.

2. **Effectiveness depends on approximating of new size of next step on current local error and current step.** Look on the methods RK4, RKF45 and B-S at (Fig. 3.3). All three methods has approximately same order, but the method of choosing new step varies. The most simple system of choosing new step by the classical methods is still better than constant step size (e.g. the RK4 with constant step size should have step size $h \sim 10^{-14}$ to integrate successfully, and thus $nE \sim 10^{11}$!), but with the respect to the embedded method or the Bulirsch-Stoer method it is not enough. The saving from optimal choosing of a new step in the B-S method is greater than fact , that it uses the Modified Midpoint method with the order 3 (in range $\lambda \in (10^{-3}, 10^{-12})$.

Figure 3.2: "Exact" solution

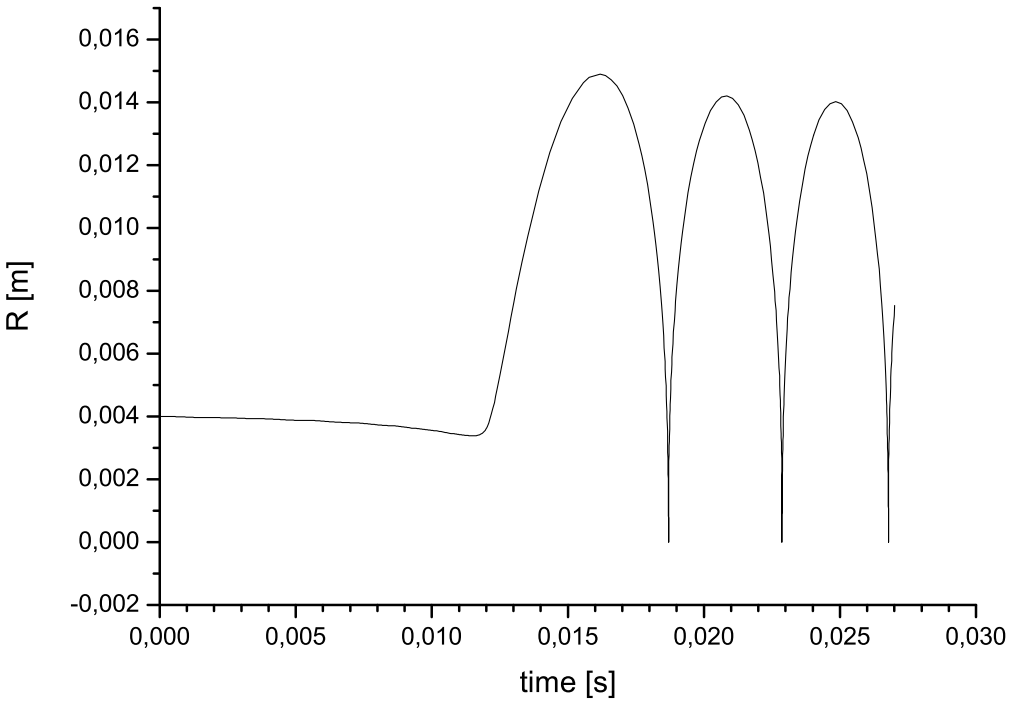

Figure 3.3: Evaluations of function vs order of global error

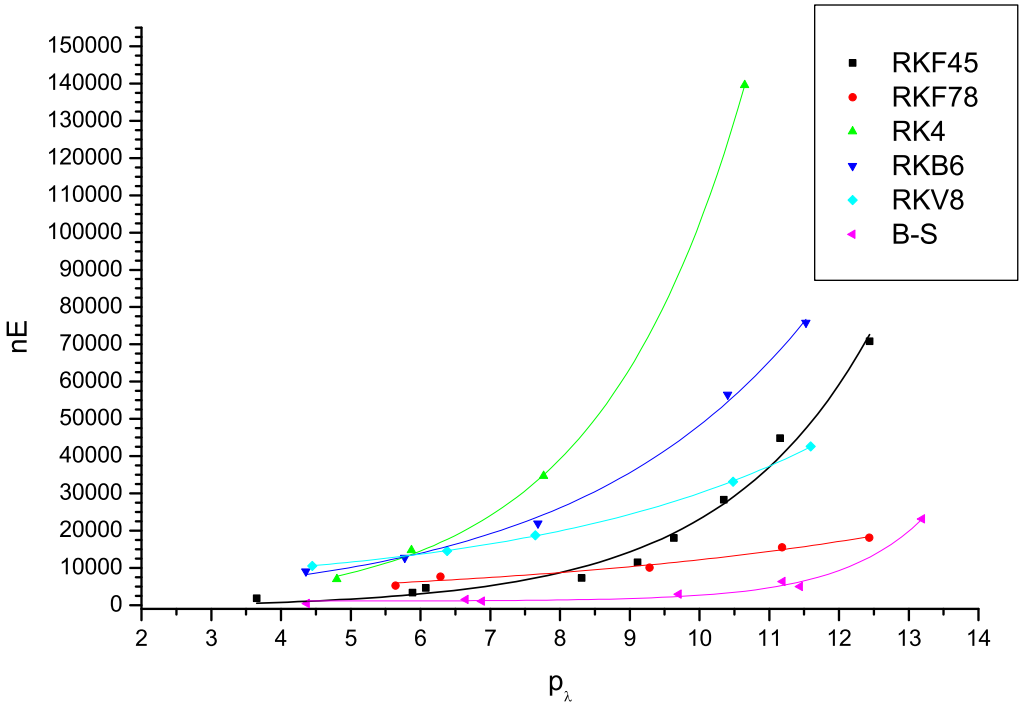

Figure 3.4: Zoom of (Fig. 3.3)

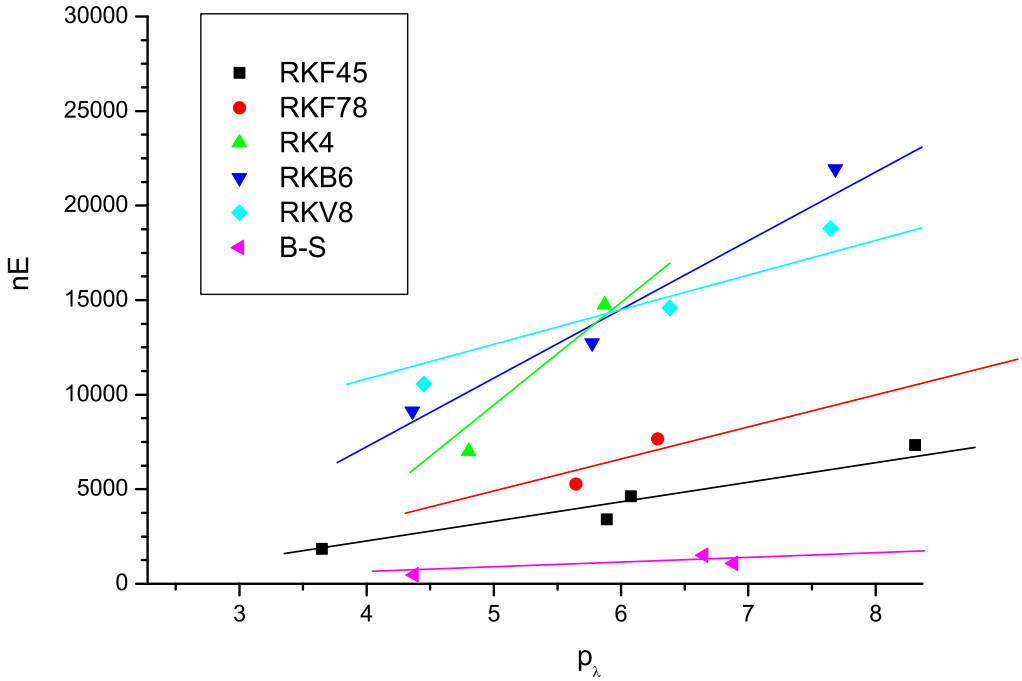

4 Remarks on Different Models

4.1 Equations

In this chapter we will discuss briefly impact of different models on the stability and speed of the numerical methods. We will compare these three methods:

1. a model proposed by equation (2.1), non-compressible liquid, isothermal $\kappa = 1$ (see previous chapters)

2. Rayleigh-Plesset equation compressible the liquid, details in [4], other parameters same as in the first model

$$\begin{aligned} \frac{d^2R}{dt^2} &= -\frac{1}{R}\Big(\frac{3}{2}\left(\frac{dR}{dt}\right)^2 + \frac{4\mu}{R}\frac{dR}{dt} + \frac{2\sigma}{\rho R}\left(1 - \left(\frac{R_0}{R}\right)^{3\kappa-1}\right) + \\ &\quad + \frac{R}{\rho c}\frac{d}{dt}\left(p_g - p_\infty\right) - \frac{p_v + p_g - p_\infty}{\rho}\Big) \end{aligned} \tag{4.1}$$

3. model proposed by the equation (2.1), non-compressible liquid, but the adiabatic approximation with $\kappa = 1,4$

4.2 Results

We used RKF45. The results can be found in Appendix C, (Tab. C.5). As we mentioned before, in use of the isothermal model, the failure of computation happens with the initial radiuses more that critical value $R_{0critical} \simeq 10^{-3}$, see (Fig. 4.1). By the failure of the computation we consider decrease of time step below reliability of the double precision.

We remind, that this value *depends* on used pressure in the infinity! With some other pressure in the infinity, the method can hold for whole range of physical reasonable radiuses. Other example of the failure of the method in literature is in work of Qin and Alehossein [5]. The solution for successive calculation can be to increase accuracy of the computing (from double to even higher) or use some scalingreduction. However, the output would not be physically acceptable, because the radius of the bubble cannot decrease to impossible values (in scale of 10^{-10} or less).

In the reality, according to [3, p.107]: " A collapsing bubble becomes unstable to nonspherical disturbances, and essentially shatters into many smaller bubbles in the first collapse and rebound."

Moreover, in the work of Qin and col. [6] there are some other variations of model, which includes also conduction and radiation. These advanced models fits better to their experimental results as isothermal or adiabatic approximation.

As it is seen of (Fig. 4.2), the different models gives the different predictions of radius of the bubbles. Difference between model (4.1) and (2.1) is almost negligible, but adiabatic model ($\kappa = 1,4$) gives kvantitativeli different results. Hence it is needed to find suitable model for our typical pressure (2.5) and compare it with the experimental data from the tested pump.

From the point of the numerical analysis, the speed of method depends on minimum step. So it highly depends on used physical model. The adiabatic model

allows increase the temperature in the bubble, which creates higher pressure with comparison of the isothermal model near collapsing point (based on simple use of the ideal gas equation). This decreases minimum step size and thus increases speed of the numerical method by more than 50% (see (Tab. C.5)). Moreover, in the case of smaller radiuses (when ration of $\frac{r_{max}}{R_0}$ is higher), the adiabatic model does not failure at all (but as it is visible from (Tab. C.5), the smallest step is below the border of reliability of double presicion).

Figure 4.1: Failure of isothermal model for $R_0 = 10^{-5}$

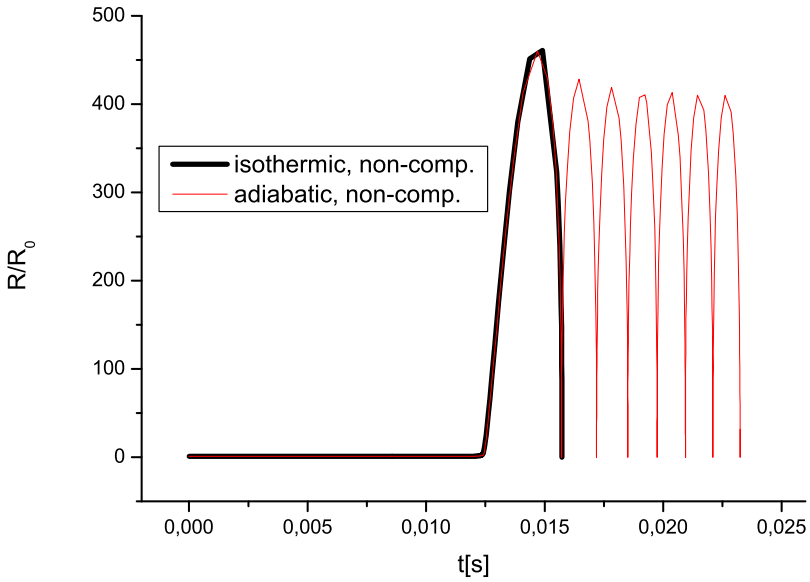

Figure 4.2: Comparison of models for $R_0 = 4 \cdot 10^{-3}$

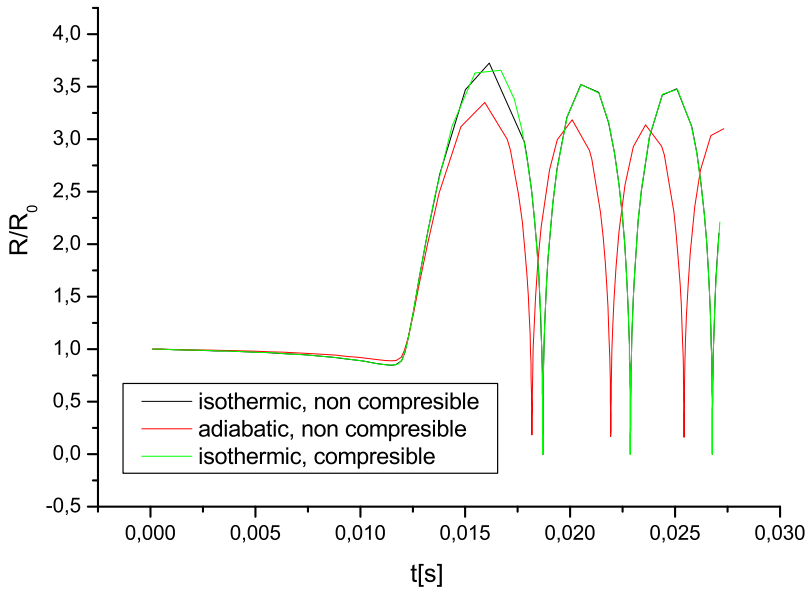

5 Conclusion

We analyzed the effectiveness and stabity of various numerical methods based on explicit one-step methods (Runge-Kutta , embedded Runge-Kutta , Bulirsch-Stoer) for solving Rayleigh-Plesset equation. The Bulirsch-Stoer method performed best, with the smallest amount of evaluation of right side and with stable solution. The embedded methods are also acceptable, but the choosing of order of the embedded method should be done in respect with the desired accuracy.

In case on medium tolerances $\epsilon < 10^{-8}$, the regularization (proposing new variable and put time as dependent variable) of the Rayleigh-Plesset equation can be used to decrease number of evaluation of right side nE. With higher tolerances regularization does not increase performance.

Global error relates with used tolerance and they are in comparable order. The investigated methods underestimates local error at collapsing points. However, global error in due to the non-stiffness of equation acceptable and solution is stable.

A physical model greatly influences speed of calculation. The isothermal model failures (radius of bubble is physically unacceptable) in case of the specific conditions and hence should be replaced by more suitable model based on varies of the temperature inside the bubble.

Next investigation should be aimed to improve of the physical model, which would give the realistic predictions for whole range of initial radiuses of the bubbles.

In the field of the numerical analysis, we did not compared the implicit numerical methods, multi-step methods and predictor-corrector methods. Especially in predictor-corrector methods there is possibility of increasing the speed of the calculation.

Bibliography

[1] Ch. E. Brennen: *Cavitation and Bubble Dynamics*, Oxford Un. Press, 1995.

[2] J.-P. Franc, J.-M. Michel: *Hydrodynamics of Pumps*, Kluwer Academic Publishers, 2004.

[3] Ch. E. Brennen: *Fundamentals of Cavitation*, Oxford Un. Press, 1994.

[4] Zima P., Sedlář M., Maršík F: *Bubble Creation in Water with Dissolved Gas: Prediction of Regions Endangered by Cavitation Erosion.*, Water, Steam, and Aqueous Solutions for Electric Power. Kyoto, Maruzen Co., Ltd., 2005, p. 232-235

[5] H. Alehossein,Z. Qin: *Numerical analysis of Rayleigh–Plesset equation for cavitating water jets*, Int. J. Numer. Meth. Engng 2007; 72:p. 780–807.

[6] H. Alehossein,Z. Qin., K. Bremhorst, T. Meyer: *Simulation of cavitation bubbles in a convergent–divergent nozzle water jet*, J. Fluid Mech. (2007), vol. 573, pp. 1–25.

[7] G. H. Goldsztein: *Collapse and rebound of a gas bubble*, Studies in Applied Mathematics,vol. 112, p. 101-132, 2004

[8] G. J. Lastman, R. A. Wentzell, A. C. Hindmarsch:*Numerical Solution of a Bubble Cavitation Problem*,J. of Comp. Physics , 28, 56-64, 1978

[9] W. H. Press, S. A. Teukolsky, W. T. Vetterling, B. P. Flannery:*Numerical Recipes in C, The Art of Scientific Computing Second Edition*,Cambridge Univ. Press, 1992

[10] A. Quarteroni, R. Sacco, F. Saleri:*Numerical Mathematics*,Springer, 2000

[11] L. F. Schampine:*Numerical solution of ordinary differential equations*,Champman & Hall, Inc. , 1994

[12] www page:*http://mymathlib.webtrellis.net/diffeq.html*,last visit 30.4.2008

A Derivation of the Reyleigh-Plesset Equation

"From a historical viewpoint, the the liquid motion induced by a spherical cavity in a infinite medium under uniform pressure at infinity seems to have been first considered by Besant in 1859. It was solved for a non-viscous the liquid by Reyleigh (1917) to interpret the phenomenon of cavitation erosion. Plesset considered the general case of bubble evolution for a viscous and non-compressible the liquid." [2, p.35]

The idea is to use the Navier-Stokes equations to derive the Rayleigh-Plesset equation , thus find function of the radius of a bubble R(t), where t is the time, in the liquid. We will follow Brennen [1, p. 47-50].

Main assumptions are following:

- bubble is spherical with fixed centre and not interacting with other bubbles
- uniform pressure variation in infinite p_∞
- constant temperature
- the liquid is incompressible (ρ - constant density) and Newtonian (μ - constant dynamic viscosity)
- gravity is neglected
- air content in bubble is constant and pressure is uniform
- there is no mass transfer through bubble border

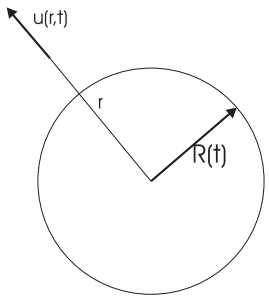

Figure A.1: Scheme

The law of mass conservation requires:

$$u(r,t) = \frac{R^2}{r^2}\frac{dR}{dt} \tag{A.1}$$

where u is the the liquid particle velocity.
The Navier-Stokes equation for motion in the r direction gives:

$$-\frac{1}{\rho}\frac{\partial p}{\partial r} = \frac{\partial u}{\partial t} + u\frac{\partial u}{\partial r} - \nu\left[\frac{1}{r^2}\frac{\partial}{\partial r}\left(r^2\frac{\partial u}{\partial r}\right) - \frac{2u}{r^2}\right] \tag{A.2}$$

where ν is the kinematic viscosity
Substitution of (A.1) to (A.2) leads to

$$-\frac{1}{\rho}\frac{\partial p}{\partial r} = \frac{2R}{r^2}\left(\frac{dR}{dt}\right)^2 + \frac{R^2}{r^2}\frac{d^2R}{dt^2} - \frac{2R^4}{r^5}\left(\frac{dR}{dt}\right)^2 \tag{A.3}$$

Integrating (A.3), under assumption $p = p_\infty$ at $r = r_\infty$, and substituting ($r = R$) leads to the equation on the bubble surface :

$$\frac{p_{r=R} - p_\infty}{\rho} = R\frac{d^2R}{dt^2} + \frac{3}{2}\left(\frac{dR}{dt}\right)^2 \tag{A.4}$$

Consider a control volume consisting of a small and infinitely thin lamina containing a segment of interface between the bubble and the the liquid. The forces acting on

this segment of lamina are the inner bubble pressure p_B, the normal stress σ_{rr} , and the surface tension σ. The equilibrium force equation in the radial r direction can be written as:

$$p_B + \sigma_{rr} - \frac{2\sigma}{R} = 0 \tag{A.5}$$

The value of the normal radial stress at the boundary $r = R$ is $\sigma_{rr} = -(p)_{r=R} + 2\mu\frac{\partial u}{\partial r}$ (μ is dynamic viscosity) and thus net force is

$$p_B - (p)_{r=R} - \frac{4\mu}{R} - \frac{2\sigma}{R} = 0 \tag{A.6}$$

Substituting (A.6) into (A.4) finally leads to Rayleigh-Plesset equation.

$$\frac{p_B(t) - p_\infty(t)}{\rho} = R\frac{d^2R}{dt^2} + \frac{3}{2}\left(\frac{dR}{dt}\right)^2 + \frac{4\mu}{R}\frac{dR}{dt} + \frac{2\sigma}{\rho R} \tag{A.7}$$

More detailed computation can be found e.g. in [5, appendix A].

B Used Numerical Methods

B.1 the Runge-Kutta Methods

Structure and derivation of the Runge-Kutta methods can be found on literature, e.g. [9], [10]. In our paper, we use coefficients for Butcher array from web site [12]. Coefficients $\{a_{ij}\}$,$\{b_i\}$ and $\{c_i\}$ from Butcher array fully characterizes the Runge-Kutta method:

$$y_{n+1} = y_n + h\left(\sum_{k=1}^{s} b_i K_i\right) \tag{B.1}$$

$$K_i = f\left(t_n + c_i h, y_n + h\sum_{j=1}^{i-1} a_{ij} K_j\right) \tag{B.2}$$

where y_n is the calculated solution of differential equation with right side f with exact solution $y(t)$ and s detonates number of stages of the method
Paraphrasing [10, p. 508-512]: Runge-Kutta methods maintain the structure of one-step method, and increase their accuracy at the price on an increase of functional evaluations at each time level, thus satisfying linearity.After assumption that $c_i = \sum_{k=1}^{s} a_{ij} i = 1, ..., s$, the sufficient condition for consistency of Runge-Kutta is that $\sum_{k=1}^{s} b_i = 1$. For one-step method, consistency implies stability and, it turn convergence. An explicit s-stage method cannot have order p greater than s, but this is an upper bound that is realized only for $s \leq 4$. Moreover, order of method in the scalar case does not necessary coincide with that in vector case(system of ODE).

1. **Classical**

   Error is calculated by technique of step doubling. Idea is to calculate approximate solution with one step h and with two steps $\frac{h}{2}$, (u_h,$u_{2*h/2}$) respectively. Then the error is

   $$\epsilon = \frac{u_h - u_{2*h/2}}{(2^p - 1)}$$

   Detailed explanation and derivation can be found e.g. in [9, p. 715].

   In error is higher than tolerance tol, we reduce the stepsize to half, if error is less that $\frac{tol}{(2^p-1)}$, we double stepsize.

2. **Embedded**

   The embedded methods calculates its error with less computational time that step doubling. We use tho different Runge-Kutta methods with s-stages of order p and $p+1$, with same set of values K_i. We approximates error $ErrR$ by difference of approximate solutions of these two methods.

   For choosing best next step, we use the method proposed in [9], which stands on order p of used method. In general case we set new value of step (but we restrict change by save factors 4 at top (if $4 < \frac{h_{new}}{h}$ then $h_{new} = 4h$) and by factor $0,1$ at down.):

$$h_{new} = 0,8h \left(\frac{tol}{err} \right)^p$$

B.2 the Bulirsch-Stoer Method

The idea is to consider approximate solution or the modified midpoint method as itself being an analytic function of stepsize h. We do the calculation with various values of h(sequence h,$h/2$,$h/4$,$h/8$,...) to the same point. Then we do polynomial extrapolation(also rational extrapolation can be used, see [9, p.725]) to $h = 0$ and determine error as error of the extrapolation. When the error is below our tolerance, we stop dividing interval and begin next step (in our case we stop at 8 times division). Next idea is to use a method whose error function is strictly even, allowing the rational function or polynomial approximation to be in terms of the variable h^2 instead of just h.

The best strategy now known is due to Deuflhard, described in [9, p. 727], which is based on evaluating work per h unit and choosing step with minimum work.

B.3 List of the Methods (Abbreviations)

Table B.1: List of used methods

Classical			
abbreviation	full name	order	# stages
Euler	Euler's Method	1	2
Mod. Mid.	Modified Midpoint Method	3	5
rk4	Runge-Kutta 4	4	4
rkn5	Nystrom's Runge-Kutta Method	5	12
rkb6	Butcher's Runge-Kutta Method	6	7
rkv8	Verner's Runge-Kutta Method	8	11
Embedded			
abbreviation	full name	order	# stages
rkf34	Fehlberg's 34 Runge-Kutta Method	3	5
rkf45	Fehlberg's 45 Runge-Kutta Method	4	6
rkf56	Fehlberg's 56 Runge-Kutta Method	5	8
rkf78	Fehlberg's 78 Runge-Kutta Method	7	13
rkpd45	Prince-Dormand's 45 R.-K. Method	4	7
rkv56	Verner's 56 Runge-Kutta Method	5	8
rkv67	Verner's 67 Runge-Kutta Method	6	10
rkv78	Verner's 78 Runge-Kutta Method	7	13
rkv89	Verner's 89 Runge-Kutta Method	8	16
Bulirsch-Stoer			
abbreviation	full name	order	# stages
B-S	Bulirsch-Stoer Method	3	3-10

where order stands for order of accepted approximate solution, # stages for number of evaluations of right side to get approximate solution and error estimate. In case of the B-S method order in table is order of the used Modified Midpoint method and number of stages varies during calculation (depends on number of division of interval h)

C Numerical Data

nE - number of evaluations of right side of Rayleigh-Plesset equation (2.1), nP - number of accepted steps by method, nO - number of rejected steps by method,ϵ-used tolerance, $\overline{\theta}$- mean value of ration of estimated local error and real, θ_{max}-maximum value of same ration, $\epsilon_{real} = \epsilon \cdot \overline{\theta}$, $p_{\epsilon_{real}} = -\frac{LOG(\epsilon_{real})}{LOG(10)}$, λ- global error

Table C.1: Output Data Classical

name	nE	nP	nO	ϵ	$\overline{\theta}$	θ_{max}	ϵ_{real}	$p_{\epsilon_{real}}$	λ	p_λ	$\frac{p_\lambda}{p_{\epsilon_{real}}}$
euler	27804	4633	4635	1,0E-04	1,55	9,2	1,6E-04	3,8	2,8E-04	3,5	0,9
mod mid	7685	1345	192	1,0E-04	1,03	8,7	1,0E-04	4,0	4,4E-06	5,4	1,3
mod mid	158425	29247	2438	1,0E-08	1,31	9,3	1,3E-08	7,9	7,2E-08	7,1	0,9
rk4	6996	417	166	1,0E-04	1,10	16,3	1,1E-04	4,0	1,6E-05	4,8	1,2
rk4	14748	939	290	1,0E-06	1,20	15,6	1,2E-06	5,9	1,3E-06	5,9	1,0
rk4	34620	2321	564	1,0E-08	1,19	16,0	1,2E-08	7,9	1,7E-08	7,8	1,0
rk4	139536	9323	2305	1,0E-11	0,89	2,0	8,9E-12	11,1	2,2E-11	10,6	1,0
rkn5	7902	295	144	1,0E-04	0,83	14,6	8,3E-05	4,1	5,0E-05	4,3	1,1
rkn5	13878	602	169	1,0E-06	0,95	10,5	9,5E-07	6,0	1,5E-06	5,8	1,0
rkn5	26604	1233	245	1,0E-08	1,16	15,0	1,2E-08	7,9	4,1E-08	7,4	0,9
rkb6	9135	282	153	1,0E-04	1,96	51,6	2,0E-04	3,7	4,4E-05	4,4	1,2
rkb6	12747	450	157	1,0E-06	3,72	55,3	3,7E-06	5,4	1,7E-06	5,8	1,1
rkb6	21945	864	181	1,0E-08	5,39	58,7	5,4E-08	7,3	2,1E-08	7,7	1,1
rkb6	56574	2326	368	1,0E-11	0,89	2,0	8,9E-12	11,1	3,9E-11	10,4	0,9
rkb6	75810	3123	487	1,0E-12	0,89	2,0	8,9E-13	12,1	3,0E-12	11,5	1,0
rkbv8	10560	190	130	1,0E-04	5,75	284,9	5,8E-04	3,2	3,6E-05	4,4	1,4
rkbv8	14586	286	156	1,0E-06	2,52	236,1	2,5E-06	5,6	4,1E-07	6,4	1,1
rkbv8	18777	423	146	1,0E-08	4,56	251,0	4,6E-08	7,3	2,3E-08	7,6	1,0
rkbv8	33165	835	170	1,0E-11	0,89	2,0	8,9E-12	11,1	3,3E-11	10,5	0,9
rkbv8	42570	1106	184	1,0E-12	0,89	2,0	8,9E-13	12,1	2,6E-12	11,6	1,0

Table C.2: Output Data Embedded

name	nE	nP	nO	ϵ	$\overline{\theta}$	θ_{max}	ϵ_{real}	$p_{\epsilon_{real}}$	λ	p_λ	$\frac{p_\lambda}{p_{\epsilon_{real}}}$
rkf34	4325	569	296	1,0E-04	2,23	37,4	2,2E-04	3,7	2,5E-07	6,6	1,8
rkf34	19620	3881	43	1,0E-08	0,17	3,0	1,7E-09	8,8	4,5E-10	9,3	1,1
rkf45	1848	221	87	1,0E-03	0,56	2,0	5,6E-04	3,3	2,2E-04	3,6	1,1
rkf45	3408	390	178	1,0E-04	0,60	38,4	6,0E-05	4,2	1,3E-06	5,9	1,4
rkf45	4626	542	229	1,0E-05	0,44	10,1	4,4E-06	5,4	8,4E-07	6,1	1,1
rkf45	7338	1178	45	1,0E-07	0,56	2,5	5,6E-08	7,3	4,9E-09	8,3	1,1
rkf45	11496	1869	47	1,0E-08	0,46	1,8	4,6E-09	8,3	7,7E-10	9,1	1,1
rkf45	18030	2960	45	1,0E-09	0,44	1,9	4,4E-10	9,4	2,3E-10	9,6	1,0
rkf45	28350	4686	39	1,0E-10	0,42	2,0	4,2E-11	10,4	4,5E-11	10,3	1,0
rkf45	44814	7425	44	1,0E-11	0,41	1,8	4,1E-12	11,4	7,0E-12	11,2	1,0
rkf45	70860	11763	47	1,0E-12	0,41	1,5	4,1E-13	12,4	3,7E-13	12,4	1,0
rkpd45	4123	396	193	1,0E-04	0,30	30,3	3,0E-05	4,5	1,5E-05	4,8	1,1
rkf56	4208	373	153	1,0E-04	0,28	1,5	2,8E-05	4,6	3,7E-06	5,4	1,2
rkf56	8816	1071	31	1,0E-08	0,37	1,3	3,7E-09	8,4	4,0E-09	8,4	1,0
rkv56	4864	416	192	1,0E-04	0,23	1,4	2,3E-05	4,6	8,2E-07	6,1	1,3
rkv67	5220	353	169	1,0E-04	0,46	2,0	4,6E-05	4,3	3,0E-06	5,5	1,3
rkf78	5278	273	133	1,0E-04	0,84	18,3	8,4E-05	4,1	2,3E-06	5,6	1,4
rkf78	7657	373	216	1,0E-06	2,47	34,7	2,5E-06	5,6	5,2E-07	6,3	1,1
rkf78	10049	508	265	1,0E-08	0,21	1,3	2,1E-09	8,7	5,2E-10	9,3	1,1
rkf78	15561	826	371	1,0E-10	0,23	2,0	2,3E-11	10,6	6,5E-12	11,2	1,1
rkf78	18148	1369	27	1,0E-12	0,30	1,1	3,0E-13	12,5	3,7E-13	12,4	1,0
rkv78	5564	290	138	1,0E-04	0,23	1,9	2,3E-05	4,6	1,4E-06	5,8	1,3
rkv89	8128	339	169	1,0E-04	0,10	3,6	9,6E-06	5,0	1,4E-06	5,9	1,2

Table C.3: Output Data Bulirsch-Stoer

name	nE	nP	nO	ϵ	$\overline{\theta}$	θ_{max}	ϵ_{real}	$p_{\epsilon_{real}}$	λ	p_λ	$\frac{p_\lambda}{p_{\epsilon_{real}}}$
B-S	5280	474	186	8,0E-03	4,2E-03	0,0	3,4E-05	4,5	4,2E-05	4,4	1,0
B-S	12936	1078	539	1,0E-03	1,1E-03	0,0	1,1E-06	6,0	1,3E-07	6,9	1,2
B-S	18016	1500	752	1,0E-04	6,5E-03	0,1	6,5E-07	6,2	2,2E-07	6,7	1,1
B-S	35240	2930	1475	5,0E-05	8,3E-05	0,0	4,1E-09	8,4	2,0E-10	9,7	1,2
B-S	60144	5004	2514	1,0E-05	1,2E-05	0,0	1,2E-10	9,9	3,6E-12	11,4	1,2
B-S	75832	6306	3173	5,0E-06	8,2E-06	0,0	4,1E-11	10,4	6,4E-12	11,2	1,1
B-S	278128	23165	11601	1,0E-07	6,3E-07	0,0	6,3E-14	13,2	6,4E-14	13,2	1,0

Table C.4: Output Data Scaling and Regularizing

name	nE	nP	nO	ϵ	$\overline{\theta}$	λ
rkf45 (3.1)	3408	390	178	1,0E-04	0,60	1,3E-06
rkf45 (3.2)	3492	400	182	1,0E-04	0,41	3,1E-06
rkf45 (3.5)	1806	265	36	1,0E-04	0,87	3,0E-06
rkf45 (3.1)	11496	1869	47	1,0E-08	0,46	7,7E-10
rkf45 (3.2)	11520	1874	46	1,0E-08	0,47	6,9E-10
rkf45 (3.5)	10944	1780	44	1,0E-08	0,52	6,0E-09
rkf45 (3.1)	70860	11763	47	1,0E-12	0,41	3,7E-13
rkf45 (3.2)	70866	11767	44	1,0E-12	0,41	3,7E-13
rkf45 (3.5)	76872	12773	39	1,0E-12	0,53	4,1E-12

Table C.5: Different models

name	R_0	nE	ϵ	h_{min}	$\frac{r_{max}}{R_O}$	method
rkf45	0,004	7657	1,00E-06	3,71E-14	3,7	1(non-comp.+isot.)
rkf45	0,004	2756	1,00E-06	5,66E-07	3,3	3(non-comp.+adiab.)
rkf45	0,004	7722	1,00E-06	3,79E-14	3,7	2(comp.+isot.)
rkf45	0,003	10699	1,00E-06	1,68E-18	4,2	1(non-comp.+isot.)
rkf45	0,003	3978	1,00E-06	1,98E-07	3,7	3(non-comp.+adiab.)
rkf45	0,003	10647	1,00E-06	1,56E-18	4,2	2(comp.+isot.)
rkf45	0,00005	52284	1,00E-04	1,00E-30	460,9	1(non-comp.+isot.)
rkf45	0,00005	62190	1,00E-04	2,31E-25	460,1	3(non-comp.+adiab.)

where r_{max} is maximum radius of bubble during whole computation